TOWARD A GOVERNING MECHANISM OF NANOSCALE ARTICULAR CARTILAGE (PHYSIOLOGIC) LUBRICATION: SMOLUCHOWSKI-TYPE DYNAMICS IN AMPHIPHILE PROTON CHANNELS*

A. Gadomski, P. Bełdowski

Department of Physics, Institute of Mathematics and Physics
University of Technology and Life Sciences
Kaliskiego 7, 85-796 Bydgoszcz, Poland

W.K. Augé II

Department of Research and Development
NuOrtho Surgical, Inc. at the Advanced Technology & Manufacturing Center
University of Massachusetts Dartmouth, Fall River, MA 02723, USA

J. Hładyszowski

Department of Physical Chemistry, Wroclaw Medical University
pl. Nankiera 1, 50-140 Wrocław, Poland

Z. Pawlak

Tribochemistry Consulting, Salt Lake City, UT 84117, USA
and
Pawel Wlodkowic University College in Płock
al. Kilińskiego 12, 09-402 Płock, Poland

W. Urbaniak

Kazimierz Wielki University
Faculty of Mathematics, Physics and Technical Sciences
Chodkiewicza 30, 85-867 Bydgoszcz, Poland
and
Technical University, Łęgska 20, 87-800 Włocławek, Poland

(Received May 29, 2013; revised version received July 12, 2013)

* Presented in part after preliminary discussions during XXV Marian Smoluchowski Symposium on Statistical Physics, Kraków, Poland, September 9–13, 2012.

Articular cartilage is an extraordinary tribochemical device designed by nature. Yet, a long-standing debate exists as to the mechanisms by which its interfacial properties facilitate lubrication toward very low static and kinetic frictional coefficients. We postulate the physiologic emergence of proton channels in amphiphile-water sub-systems undergoing mesoscopic Smoluchowski-type dynamics as a governing mechanism toward nanoscale articular cartilage lubrication. We argue that an enthalpic interplay between geometric and electrostatic confinement and the associated entropic counterpart is characteristic of proton channel crowding rather than of proton drift. A proton-wave inversion effect also supported by quantum mechanical evaluation is demonstrated such that the wave plays a beneficial role in nanoscale lubrication driven by local free-energy gradients. These findings have practical implications for the treatment of damaged articular cartilage as exemplified by the physiochemical scalpel used in modern tissue rescue interventions as a wound healing biomimic facilitating articular cartilage lesion recovery. Amphiphile proton channels also provide a mechanism for surface active phospholipid self-assembly supportive of their efficacy as an occasional sacrificial layer designed to mitigate certain perturbation events. This behavior remains a necessary requisite to reconstitute normal bearing surfaces after therapeutic tissue rescue.

DOI:10.5506/APhysPolB.44.1801
PACS numbers: 82.70.Uv, 87.14.Cc, 47.85.mf, 68.35.Fx

1. Introduction

Understanding mechanisms responsible for the interfacial properties of articular cartilage (AC) surfaces has long been sought due to their remarkable performance capabilities and because their dysfunction contributes to the disease burden of conditions such as osteoarthritis. Recently, the role of the proton and its attendant protonation potential has been discussed as a unifying feature in AC therapeutics [1]. Observations such as decreased synovial fluid pH commensurate with damage, interfacial structured water proton gradient formation adjacent to hydrophilic biosurfaces, damaged tissue disaggregation during arthroscopic lavage, and debris delivery mechanisms for synovial phagocytosis all reflect aspects of interfacial proton dynamics at AC surfaces. Such protic observations inspired the therapeutic application of redox magnetohydrodynamic technology to AC surfaces in order to create protonation potentials mimicking the azurophilic degranulation respiratory burst myeloperoxidase system of polymorphonuclear granulocytes during the acute phases of wound healing [2, 3]. In the form of a physiochemical scalpel, this technology created the therapeutic discipline of tissue rescue that is now being applied to AC lesions [4].

The present study considers further the protic phenomena at AC surfaces in the properties of nanoscale proton channels within amphiphilic structures as a governing mechanism for AC lubrication (Fig. 1). The surface active phospholipid layer (SAPL) is a nanoassembly displaying oligolamellar amphiphilic structures on AC surfaces judged by many to participate in boundary lubrication regimes through synergistic mechanisms with other synovial fluid constituents [1, 5–9]. The SAPL effectively manages ambi-

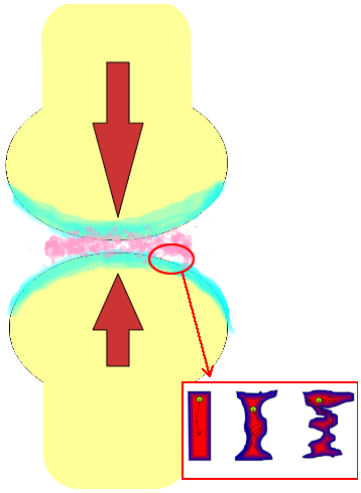

Fig. 1. Schematic representation of a synovial joint organ system consisting of two poroelastic surfaces within a fluid milieu. The insert represents three types of ion channels postulated in the mesoscopic non-equilibrium thermodynamic model of facilitated lubrication presented in this study.

ent pH and associated protonation potentials [7], an attribute deployed as a trait-targeting method to selectively deliver engineered irrigant protonation potentials [10] to AC lesions that lack geographic SAPL coverage. Because amphiphiles exhibit self-assembly behaviors, the SAPL is often viewed as an occasional sacrificial layer that mitigates certain perturbation events and subsequently reforms. Hence, the reconstruction of normal bearing surfaces after therapeutic tissue rescue is achievable provided that a suitable substrate is created upon which SAPL lamina can reconstitute (Fig. 2). Tissue rescue protonation potentials have been modeled as a biophysical battery based upon the inverse mass ratio derived from Lorentzian charge-to-mass calculations useful for titrating therapeutic effects *in vivo* [3]. As the ambient aqueous milieu of AC surfaces and SAPL aggregation–disaggregation dynamics display protic relationships, further modeling expanding Lorentzian charge-to-mass ratio calculations have provided additional insights into the boundary lubrication behaviors of AC [11].

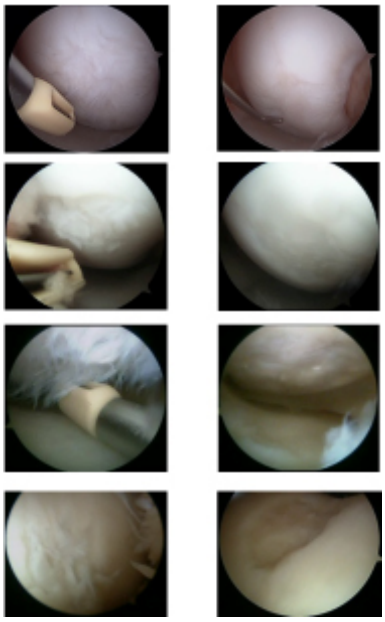

Fig. 2. Tissue rescue for the articular cartilage lesions associated with osteoarthritis. Intraoperative digital photographs of pre-treatment (left) and post-treatment (right) lesions with various grades of articular cartilage damage advancing from top to bottom. The physiochemical scalpel is designed to achieve nanometer resection precision, increased cell-to-matrix enrichment ratios, and induction of tissue assembly transcriptional responses in tissue subadjacent to the wound bed. Note the resultant decrease in surface roughness which can allow SAPL nanoassembly lamina to re-form toward a better bearing surface [5–7]. Reproduced with permission [1].

Inherent to the formation of a protonation potential is proton movement. Molecular dynamic simulations reveal that proton movement near phospholipid surfaces is generally more inhibited than augmented [12]. For example, lateral proton conductance is equally limited at low ambient pH in bilayers formed from protonatable phospholipids and those formed from covalently modied phospholipids that cannot be protonated [13]. Further, differences in proton conductance at higher pH are fully described by electrostatically induced changes in local proton concentration near phospholipid membranes [14]. Such results provide little evidence of significant lateral proton conduction as a mechanism for the observed management of ambient pH and associated protonation potentials by the SAPL and is consistent with the unique properties of interfacial water at phospholipid surfaces [15]. Interfacial water is often less mobile, more ordered, and crystalline-like, constraining negative charges but allowing protons to move more freely in bulk solution. Such interfacial behavior also manifests in colloidal and polymer

biomatter aggregation–disaggregation dynamics through the well-recognized mechanism of pore channel formation in a manner similar to the electric double layer phenomenon.

Because water plays a prominent role [10] in AC function and phospholipid proton channels [16], the very rapid structural diffusion of protons in water itself [17] merits brief discussion since interfacial water often excludes solutes [18] that might consequently influence proton movement. The Grotthuss proposal has provided a useful conceptual framework to describe general prototropic transfer by hoping from one water molecule to the next and accompanied by water molecule reorientation. The actual transfer mechanism remains a subject of some debate [12, 19] particularly because the identity of the conducted proton may change [20] and the recipient water molecule may reorient in the hydronium donor field [21]. Water is a very suitable medium for proton conduction because of its propensity to form hydrogen bonds whereby the hydrogen-bonded network can delocalize solvated protons. Proton transport is determined by the rate at which hydrogen bonds between a hydronium ion and a water molecule form, which when considering the hydrogen bond flicker rate of femto- to pico-second levels [22], is a very rapid process. It has further been proposed that proton mobility is higher than other ions because contraction of the O–O bond distance adds energy to hydroxide transfer [23] and the additional kinetic energy of the excess proton increases the energy of hydronium ions [12].

The purpose of the present study is to describe the dynamic organization of nanoscale amphiphilic matter at AC surfaces based upon drift velocity in corresponding Smoluchowski-type convection–diffusion equations as a further manifestation of interfacial protic phenomena.

2. Amphiphile proton channel model basics

The proposed model is based on mesoscopic non-equilibrium thermodynamic (MNET) working schemes that have been well established for colloid- and polymer-type biomatter aggregation dynamics [24, 25]. In general terms, the model is based on a set of equations that govern system thermodynamics at the physical mesoscale. Accordingly, the drift velocity in MNET is given as follows [26]

$$v_d = -\frac{d\Phi}{dx}\,\frac{D}{k_{\mathrm{B}}\,T}\,, \tag{1}$$

in which D is the diffusion constant, $\Phi \equiv \Phi(x)$ Gibbs' free energy at a space coordinate x and k_{B} and T are Boltzmann's constant and temperature, respectively. The flux in the MNET Smoluchowski-type systems [25] reads

$$J(x,t) = -D\frac{\partial}{\partial x}P(x,t) + v_d\,P(x,t)\,, \tag{2}$$

rendering the local continuity equation to be obeyed by $P(x,t)$ in the form

$$\frac{\partial}{\partial t}P(x,t) = D\frac{\partial^2}{\partial x^2}P(x,t) - \frac{\partial}{\partial x}(v_d P(x,t))\,. \tag{3}$$

One can then specify the Gibbs' entropy postulate [26] in a γ-space as follows $S = S_{\rm eq} - k_{\rm B}\int P(\gamma,t)\ln\frac{P(\gamma,t)}{P_{\rm eq}(\gamma)}d\gamma$, wherein the specification holds here for $\gamma = x$. Here, $S_{\rm eq}$ is the entropy of the system at equilibrium, while $P(\gamma,t)$ and $P_{\rm eq}(\gamma)$ stand for the probability density of finding the system at state γ at time t in the former case or at equilibrium in the latter.

The stationary (or, steady) timeless state [27] of Eq. (3) is defined as

$$J \equiv J(x,t) = \text{const.} \geq 0\,, \tag{4}$$

which follows from $\frac{\partial P(x,t)}{\partial t} = 0$. This single state renders the stationary solution to Eq. (3) of the well known Boltzmann-like form such as $P_{\rm eq}(x) \simeq \exp\left[\frac{-\Delta\Phi}{k_{\rm B}T}\right]$. It means that, in principle, it is expected for the system to have one decisive barrier $\Delta\Phi$ to overcome.

3. Amphiphile channels undergo confinement/crowding involving proton-waves

MNET provides a general framework from which one can study the dynamics of systems defined at a coarse-grained mesoscopic level that has been used to analyze various processes [13, 14, 28, 29].

3.1. Geometric confinement of the proton channel

Let us begin with the Gibbs' free energy Φ in a classic form

$$\Phi = H_{\rm el} - T\,S\,, \tag{5}$$

where enthalpy $H_{\rm el}$ is associated with the pressure $p(x)$ exerted by the protons' wave on the channel's far-end cross section, made up of negatively charged amphiphiles. The elementary change of $H_{\rm el}$, corresponding to some infinitesimal volume dV in which a part of H^+-wave resides, is given by

$$dH_{\rm el}(x) = p(x)dV\,. \tag{6}$$

The infinitesimal volume of the channel is taken as

$$dV = l_{\rm ch}\,dA(x)\,, \tag{7}$$

where $l_{\rm ch}$ is its length, taken as a constant, and $A(x)$ is a cross-section area of the channel, varying with space coordinate x, *cf.* Fig. 3. The figure

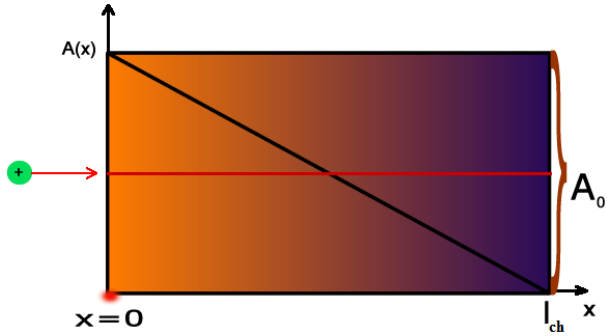

Fig. 3. Ion channel of length l_{ch}. The diagonal line when crossing the channel of length l_{ch}, having the entrance cross-section area of A_0, shows a systematic confinement to ion passages, viewed from left (maximum passage) to right (zeroth passage). At the beginning, the free movement of ions is allowed. However, the closer to the right end of the channel, the movement of ions along the length of channel becomes impossible [29]. For analytical depiction of the (linear) confinement, *cf.* (15).

represents the proton channel under a geometrical confinement. Then one obtains a formula for dH_{el}

$$dH_{\mathrm{el}}(x) = F_{\mathrm{el}}\, l_{\mathrm{ch}}\, A^{-1}(x)\, dA(x)\,, \tag{8}$$

assuming a constant local electric attraction field, $F_{\mathrm{el}} = \mathrm{const.}$, between H^+-wave and the negatively charged amphiphile. Moreover, the H^+-channel (Fig. 4) (non)equilibrium entropy S and area $A(x)$ relate to each other as

$$S_{\mathrm{eq}}\, A(x) = S(x)\, A_0\,, \tag{9}$$

where $A_0 = \mathrm{const.}$, *cf.* (Fig. 3), is the maximum cross-section area depicted at the left-hand side end of the channel. Thus an equality, expressing the cross section *versus* entropy local balance

$$S_{\mathrm{eq}}\, dA(x) = dS(x)\, A_0 \tag{10}$$

is postulated, and ultimately a change of nonequilibrium proton-channel (Fig. 4) entropy $dS(x)$ looks like

$$dS(x) = \frac{S_{\mathrm{eq}}}{A_0} dA(x)\,. \tag{11}$$

The form of Boltzmann entropy for N_{H^+} number of protons of concentration c_{H} is as follows

$$S_{\mathrm{eq}} = k_{\mathrm{B}} N_{H^+}\, \ln[c_{\mathrm{H}}\, A_0\, l_{\mathrm{ch}}]\,. \tag{12}$$

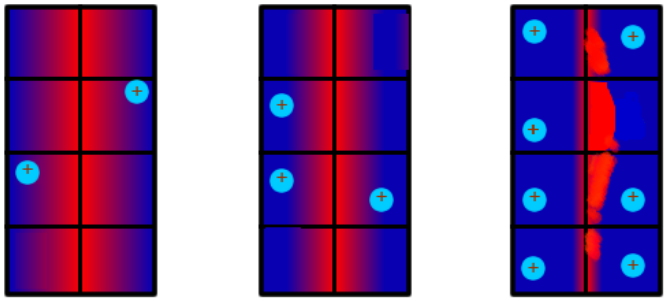

Fig. 4. Schematics of proton channel crowding. The left image depicts the least crowded type. In this case, the free movement of ions is allowed. In the middle image, the channel is more crowded, yet ions can still move to some degree. The right image depicts a channel through which ions are not allowed to pass. Gray/red represents allowed ion pathways whereas dark gray/blue represents non-allowed ion pathways.

Note that the bigger $S_{\rm eq}$ is, the lower the pH of synovial fluid [7, 11, 13] due to increasing proton crowding conditions, *i.e.* if $c_{\rm H}$ goes up at constant channel volume. Thus from relation (5), assisted by (11), we can obtain a formula

$$d\Phi(x) = \left[F_{\rm el}\, l_{\rm ch} A^{-1}(x) - T\, S_{\rm eq}\, A_0^{-1}\right] dA(x)\,. \tag{13}$$

Equation (13) is formally equivalent to

$$\frac{d\Phi(x)}{dx} = \left(\frac{F_{\rm el}\, l_{\rm ch}}{A(x)} - \frac{T\, S_{\rm eq}}{A_0}\right) \frac{dA(x)}{dx}\,. \tag{14}$$

Figure 3 shows the assumed geometry of our H^+-channel. The area of the channel changes according to a linearly decreasing function of x

$$A(x) = A_0 \left(1 - \frac{x}{l_{\rm ch}}\right)\,. \tag{15}$$

Inserting Eq. (15) to Eq. (14), upon denoting $W_{\rm el} = F_{\rm el}\, l_{\rm ch}$, one provides

$$\frac{d\Phi(x)}{dx} = -\left(\frac{W_{\rm el}}{l_{\rm ch}} \frac{1}{1 - \frac{x}{l_{\rm ch}}} - \frac{W_{\rm entr}}{l_{\rm ch}}\right)\,, \tag{16}$$

and finally,

$$\frac{d\Phi(x)}{dx} = -\frac{F_{\rm el}}{1 - \frac{x}{l_{\rm ch}}} + F_{\rm entr}\,, \tag{17}$$

wherein the entropic-force work $W_{\rm entr} = F_{\rm entr}\, l_{\rm ch}$ applies. Below, both forces will be specified in a more detailed way.

3.2. Entropic effect of crowding on the proton channel (thermo)dynamics

Thus, the entropic part of the force, provided that the protons are viewed as an ideal gas, is taken as

$$F_{\text{entr}} = \frac{k_{\text{B}}\, T\, N_{\text{H}^+}}{l_{\text{ch}}} \ln[N_{\text{H}^+}]\,. \tag{18}$$

Finally, by inserting formula (17) to (1), one gets final relation for the proton-wave velocity

$$v_d^{\text{H}^+} = \frac{D^{\text{H}^+}}{k_{\text{B}}\, T} \left(\frac{F_{\text{el}}}{1 - \frac{x}{l_{\text{ch}}}} - F_{\text{entr}} \right), \tag{19}$$

wherein it has been emphasized that $D = D^{\text{H}^+}$ due to diffusion characteristics of protons, *i.e.* that protons are prone to diffuse either directionally or non-directionally, thus, undergoing sometimes a standard random walk.

From Eq. (19), being generally x-dependent, it follows that there can be three distinct cases analyzed, that when associated with Fig. 3, can be evaluated as follows.

First, if in Eq. (19) at $x \simeq 0$, *i.e.* in the left end of the channel, Fig. 3, one provides that

$$v_d \simeq (F_{\text{el}} - F_{\text{entr}}) \frac{D^{\text{H}^+}}{k_{\text{B}}\, T}\,, \tag{20}$$

this way anticipating a constant, and for $F_{\text{el}} > F_{\text{entr}}$ positive value of the proton-wave velocity, v_d, implying a domination of electric forces over their entropic counterpart. If, in turn, $F_{\text{el}} < F_{\text{entr}}$, and the entropic part of the force would prevail, the H^+-wave steps back due to proton overcrowding, even in the most broad part of the channel. Thus, a proton wave inversion effect is observed under loading conditions.

In order to further characterize this proton wave inversion effect, let us consider the value of proton flux velocity. As discussed in previous models [3], there are about $n_{\text{L}} = 4$ to 8 lamellae on the surface of normal AC in various locations, ranging from 6–10 nm in thickness each. If one takes $n_{\text{L}} = 6$, then the value of proton channel length can be taken as $l_{\text{ch}} = 60$ nm. The proton mobility is given by $\mu = \frac{D^{\text{H}^+} e^{\text{H}^+}}{k_{\text{B}}\, T}$ which leads to 36.3×10^{-8} m^2/s V, and the corresponding electric potential reads $U = -40$ mV. Let us put $N = 10^5$ protons in the channel. One can obtain $v = 30$ μm/ns $\equiv$ 30 km/s $\approx 10^{-4}$ c_{vac}; c_{vac} stands for the light speed in vacuum conditions. Then, the energy of protons is *ca.* 3.0 eV and a length of proton wave, estimated from de Broglie principle, is about 10^{-11} m, as compared to the data from [30] in which the ion-channel velocities of typical ions such as Na^+ are estimated by means of the Langevin dynamics. Our

estimation of the above data relies on some typical values, but one may also choose another dataset. The rule, however, is that if one specifies the electric potential at some value, one has to adjust the number of protons assigned to it. This physical fact is related to the need to have an adequate level of electric power to move the corresponding number of protons through the channel.

At this stage of our presentation, let us recall that the surface active phospholipid layer (SAPL) is a nanoassembly displaying oligolamellar amphiphilic structures lining AC surfaces and has been judged by many to participate in boundary lubrication regimes through synergistic mechanisms with other synovial fluid constituents. One such a synergistic mechanism can be viewed as follows. Assume that a perturbation load is applied to the system. It may cause a certain deterioration of the first lamella, requiring adjustment to the new situation. If the system is equipped with additional amphiphile molecules [31], such a load may cause their translocation, and at the same time, emergence of a new micellar structure prone to facilitate lubrication [1]. If the magnitude of the applied load is increased, then more lamellae are prone to their structural rearrangement. The result is the creation of new micelles [5, 14] contributing to the ultralow friction mechanism by means of forming new ion/proton passages amongst and within them. Thus, what we have estimated as the channel length is rather more the cumulative channel passage (overall ion-channel) of the length of an oligolamellar system, see above.

Second, if in Eq. (19) at $x \simeq l_{\mathrm{ch}}/2$, *i.e.* in the middle of the channel, (Fig. 3), one gets that

$$v_d \simeq 0\,, \tag{21}$$

assuming that a certain force threshold $F_{\mathrm{el}} \simeq F_{\mathrm{entr}}/2$ could be reached. It is feasible to manage when work $W_{\mathrm{el}} = F_{\mathrm{el}}\, l_{\mathrm{ch}} = (k_{\mathrm{B}}/2)\, T\, N_{\mathrm{H}^+} \ln[N_{\mathrm{H}^+}]$, that is to say, when the electric energy equals (almost) exactly the thermal proton-wave energy, $E_T = (k_{\mathrm{B}}/2)\, T\, N_{\mathrm{H}^+} \ln[N_{\mathrm{H}^+}]$ provided again that protons are dealt with as an ideal gas. In other words, one can say that an almost perfect mutual compensation of both main parts of the energies applies.

Third, if in Eq. (19) at $x \simeq l_{\mathrm{ch}}$, *i.e.* at the right-end of the channel, (Fig. 3), one obtains that the only dominating part remains to be the electric part of the force enhanced by the confinement $x \simeq l_{\mathrm{ch}}$. The entropic part of the force will not play any considerable role here but only the geometrical right-end channel's confinement. Thus, the velocity v_d would practically approach $v_d \approx {F_{\mathrm{el}}}^{(\infty)} \frac{D^{\mathrm{H}^+}}{k_{\mathrm{B}}\, T}$, wherein ${F_{\mathrm{el}}}^{(\infty)}$ would become a really large value of the electric force that arises under confinement. In order to arrive at finite and experimentally accessible values of v_d, it has to be assumed that D^{H^+} would drop in the period of the electric force-field action immensely. It is

plausible to accept, provided that $T = \text{const.}$ still applies, if one assumed that the protons under confinement would walk subdiffusively, their root mean-squared displacement, denoted by l_{rmsq} had to cease upon increasing time t, such as $l_{\text{rmsq}} \equiv l_{\text{rmsq}}(t) \sim t^{\mu}$ with $0 < \mu < 1/2$. In other words, the value of D^{H^+} should be assumed t-dependent, causing $D^{\text{H}^+}(t) \sim t^{2\mu-1}$ to decrease in an algebraic way [31]. Another option that one would not discard is the logarithmic (even Sinai-type or billiard-involving) diffusion which also decelerates in its tempo when compared with its standard counterpart [32]. In the present study, following others [11, 28, 31], we wish however to focus on the power-law behavior of the diffusion function.

Thus, for comparison, let us consider three cases of the prototype H^+-channel studied in [31] (Fig. 5), and being of relevance to the overall nano-tribological depiction we are addressing. When transforming previous studies [11, 31] into our present scheme with close analogy to [33], one would list them as follows. If at the first instance $x \simeq 0$, then $v_d^{\text{H}^+}(x \simeq 0) := \frac{\langle x \rangle}{t}$, where

$$\langle x \rangle \propto t^1 \tag{22}$$

would appear [11]. In the second case, if $x \simeq \frac{l_{\text{ch}}}{2}$, then $\langle x^2 \rangle$ is related with D and

$$\langle x^2 \rangle \propto t\,, \tag{23}$$

thus [31]

$$\sqrt{\langle x^2 \rangle} \propto \sqrt{t}\,, \tag{24}$$

and finally (*i.e.*, in the third case), if $\text{x} \simeq l_{\text{ch}}$, then

$$\frac{\langle x \rangle}{t} \to 0\,, \tag{25}$$

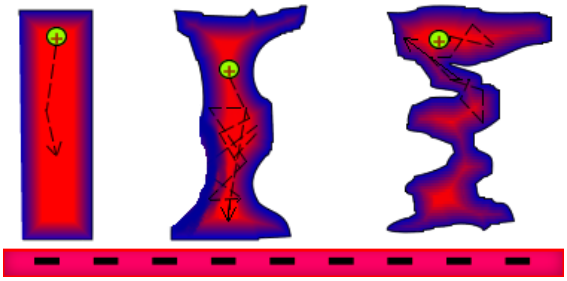

Fig. 5. Proton channel types. Ascending levels of confinement are depicted from left to right. The cathode under the channel depiction (gray/red bar with minus signs) is conceptualized as causing a constant attracting field influencing H^+ movement. The cathode is modeled as either charged phosphate groups ($-\text{PO}_4^-$) from [35] or a charged HA (hyaluronan) lattice.

consistently with a reasoning presented in [11, 31]. $\langle x^i \rangle \equiv \langle x^i(t) \rangle = \int_0^\infty x^i P(x,t)dx$ denote central moments ($i = 1, 2$) of the probability density function $P(x,t)$ from Eq. (3). We see that based on our approach to the proton channel we are able to propose a synergistic link between meso- and nanoscale considerations. The former is based upon designing the drift velocity (v_d) based on interplay between electric-field assisting confinement and entropy (over)crowding, both of which being analyzed above.

The latter relies on proposing the protons' motions bases on anomalous random walk concepts [31], and references therein. These bases, in turn, via the (extended *viz.* time-involving [31]) fluctuation-dissipation theory, address the proton (time-dependent) diffusivity in terms of the corresponding local changes of water viscosity by means of the Grotthuss-type mechanism [12] with reorientations of water dipoles, and suitable breakages of the H-bonds assisting the H^+ passages [11]. The local viscosity, in turn, can be thought of as inversely proportional to the dynamic (or, equivalently, kinetic) coefficient of friction measured for the AC system [7, 13, 31]. Such a measurement is certainly accompanied by adequate pH changes, *cf.* [1, 5, 6, 14]. Moreover, there is also another conceptual merger to be proclaimed based on the approach proposed. It is due to having a complete analogy between the friction coefficient μ_d and the diffusion coefficient D^{H^+}, via the extended fluctuation-dissipation theorem, applicable virtually to our model AC system, namely that $\mu_d \approx D^{H^+}(t)$. According to our conceptual view, the quantity D^{H^+} can provide an approximate estimate of the Grotthuss-type conductivity for the AC biosystem under study. To be specific, based on the theorem, thus accepting that D^{H^+} is proportional to proton mobility, the latter being also proportional to the corresponding conductivity, what, in turn, determines the value of the dynamic (*viz.* kinetic) friction coefficient [11, 31]. The determination uncovers the fact that the easiest friction *viz.* maximum facilitated lubrication mode occurs when protons go with constant and sufficient velocity v_d toward negatively charged amphiphile targets. The confinement *versus* crowding property is able to spoil the maximum (nanoscale) lubrication mode by damping the enhanced protons' diffusion toward standard and subdiffusive modes. The synergistic synchronization of both the Smoluchowski-type mesoscale nonequilibrium thermodynamics mode with its nanoscale and fluctuation dissipation counterpart lies within the core of our semi-quantitative, simple proposal. Resorting either to suitably chosen sets of experimental pH-changes data, *cf.* Fig. 6, or toward designing an adequate computer simulation, terms of molecular dynamics, or even the Brownian, Langevin-type dynamics, would shed additional light on SAPL function.

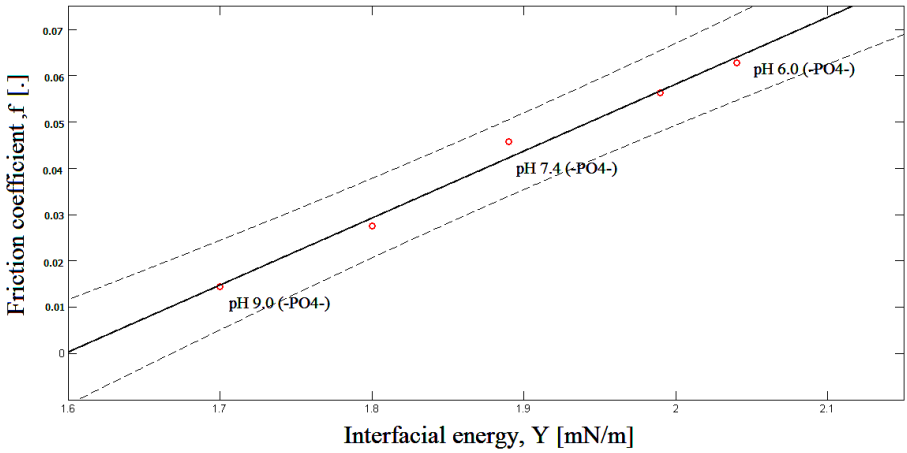

Fig. 6. Graph shows the interfacial energy *versus* coefficient of friction dependence for phosphatidylcholine (PC) bilayer surface of phosphate ($-PO_4H/-PO_4^-$) group. Over the pH range 6 to 9 phosphate group is charged ($-PO_4^-$), while the amino group (NH_2) group is neutral. The pH 7.4 is a working value when friction processes are taking place in joints. The graph is congruent to Fig. 6.9. from [35]. The pH levels seen on the graph can be correlated with outputs of Eq. (12) and/or Eq. (18), announcing that pH is an important (H^+-crowding sensitive) quantity, influencing friction-lubrication ion conditions. The linear regression (at a confidence level of 0.95) of the small data set yields $f(Y) = AY + B$, where $A = 0.1447$ m(mN)$^{-1}$, $B = -0.2312$, and f designates the friction coefficient.

4. Quantum description of proton movement in the narrowing channel

Let us consider a melted quantum mechanical description of proton moving in a SAPL channel with impermeable walls. To separate proton movement along the channel and the transversal component completely restricted by wall barrier, we take the wave function in a form

$$\psi(\phi, \rho, x) = \sum_{m,n} e^{im\phi} c_{m,n} J_m \left(\frac{\kappa_{m,n}\rho}{\rho_b} \right) f_{m,n}(x) \,, \tag{26}$$

where x is a coordinate along the channel, ρ_b is the radius of boundary, a limiting value of ρ, which is the distance from the symmetry axis of the pore; ϕ is an angle around the axis, J_m the Bessel function of integer order m, $\kappa_{m,n}$ is nth root of J_m; $f_{m,n}$ is the amplitude of proton wave function in its movement along the channel, and $c_{m,n}$ normalization coefficient of cylindric part of ψ.

Now, the problem of proton movement along the channel can be separated into the 1-D Schroedinger equation for each $f_{m,n}$ with the effective potential $U_{\mathrm{eff},m,n}(x) = \frac{\hbar^2\pi\kappa_{m,n}^2}{2MA_0}\frac{1}{1-\frac{x}{l_{\mathrm{ch}}}} - F\,x$ if the cross section of the pore is $A(x) = A_0\,(1-\frac{x}{l_{\mathrm{ch}}})$, *cf.* (15) (where M is a proton's mass).

Let us consider some chosen m and n values and parameterize the effective potential by its "entrance" value $V = \frac{\hbar^2\pi\kappa_{m,n}^2}{2MA_0}$, and a dimensionless parameter $a = \frac{Fl_{\mathrm{ch}}}{V}$ and introduce nondimensional coordinate $\zeta = \frac{x}{l_{\mathrm{ch}}}$ then, the effective potential takes a simple form

$$U_{\mathrm{eff}} = V\left(\frac{1}{1-\zeta} - a\zeta\right). \tag{27}$$

If we also scale energy by V and introduce nondimensional energy parameter $\varepsilon = \frac{E}{V}$, the values of return points are

$$\zeta_{1,2} = \frac{\varepsilon - a \mp \sqrt{(a-\varepsilon)^2 + 4a(\varepsilon-1)}}{2a}. \tag{28}$$

Now, let us estimate the transmittance coefficient D_{T} of the channel in an usual way

$$\ln D_{\mathrm{T}} = -\frac{2l_{\mathrm{ch}}\sqrt{2MV}}{\hbar}\,\Re\left(\int_0^1\left(\frac{1}{1-\zeta} - a\zeta - \varepsilon\right)^{\frac{1}{2}} d\zeta\right). \tag{29}$$

The integral in the r.h.s. of the equation can be expressed by elliptic integrals of the return points values and the real part of the integral should be taken, which is always less than 2 for nonzero energy and force thus,

$$\begin{aligned}\ln D_{\mathrm{T}} \;=\; & -\frac{2l_{\mathrm{ch}}\sqrt{2MFl_{\mathrm{ch}}}}{\hbar}\,\Re\left[\sqrt{\frac{(1-\varepsilon)V}{Fl_{\mathrm{ch}}}} + \sqrt{1-\zeta_1}\,(2-\zeta_1-\zeta_2)\right.\\ & \times E\left(\arcsin\frac{1}{\sqrt{1-\zeta_2}}, \frac{1-\zeta_2}{1-\zeta_1}\right)\\ & \left.+\sqrt{1-\zeta_1}\,(\zeta_1-\zeta_2)F\left(\arcsin\frac{1}{\sqrt{1-\zeta_2}}, \frac{1-\zeta_2}{1-\zeta_1}\right)\right].\end{aligned} \tag{30}$$

If an upper bound for the integral is applied, the estimation for D_{T} is as follows

$$D_{\mathrm{T}} \geq e^{-4\kappa_{m,n}\frac{l_{\mathrm{ch}}}{\rho_{\mathrm{b}}(0)}}, \tag{31}$$

which is the overall range of the H^+-wave transmission through the channel we have used.

The entropic force appearing in the Smoluchowski-like approach, *cf.* (18) comes a transversal confinement from localization of the proton wave. The consequence of this fact is that protons move in effective potential which is angular momentum dependent and create a finite barrier at the mouth of the channel and is infinite at its end, *cf.* Fig. 4. In analogous searching-for-target (or entrance) Smoluchowski dynamics problems, such as the ones recognizing specific targets along the DNA molecule by some active and charged (small) proteins, *cf.* [36, 37] the whole problem splits as ours to some longitudinal- and transversal-direction involvement, due to the role played by the confinement, and possibly over-crowding caused by protein effective number upon performing the complex electrostatics search. However, there is a finite transmition coefficient of a proton wave through such conus-like channels. The greater angular momentum the greater the barrier at the mouth of the channel as $\kappa_{m,n}$ grows with both of the indices m and n. This means that the confinement energy changes as the channels are steeper, causing greater forces exerted on proton. However, the forces exerted on protons are equal to the forces which protons exert on the walls. These forces and the shear may destroy the molecular structure of walls and also cause protons at energy level of ~ 1 eV to walk subdiffusively at the narrowest confinement as changes of effective potential are extremely great within the geographic hydration shells present.

5. Final address and perspective

The final address can be presented as follows:

- AC damage leads to increased disease burden largely due to lesion progression exacerbated by the loss of a normal bearing surface [34]. Such lesion sites exhibit compromised tribochemical performance capabilities because the increased surface asperities associated with interstitial matrix failure are accompanied by a lack of geographic SAPL coverage [1, 3]. The SAPL is an oligolamellar nanostructure exhibiting reverse micelle characteristics, protic aggregation–disaggregation behaviors, surface hydrophilic–hydrophobic balancing actions, and intralamellar hydration swelling features that serve to mitigate certain perturbation conditions and protect against pathologic solutes. These functions are influenced by ambient synovial fluid pH variations that impact SAPL electrical charge and frictional surface properties [14] such as that which is observed commensurate with joint organ system disease [1].

- This report presents the fundamentals of an MNET-based model envisioning a governing mechanism of AC lubrication in a thermodynamic system that is based upon proton movement and attendant protonation potentials, also benifiable by means of quantum-mechanical quantitive reasoning, *cf.* Fig. 7. The model captures the interplay between structural confinement and its counter effect during SAPL aggregation–disaggregation that we have termed the Proton Wave Crowding. Both effects contribute to a facilitated lubrication function by way of SAPL nanoscale channels due to the binding of hydrogen ions at specific sites within molecular hydration shells effecting local dynamics at nanometer distances and femto- to pico-second ranges. Because the Smoluchowski dynamics have been utilized by others in the context of polymeric dispersive aggregations and their motions [38, 39], we have utilized the concept of random walk to limit partial differential equations for standard and time-dependent functions as has been applied to colloid dispersions in swollen polymer matrices.

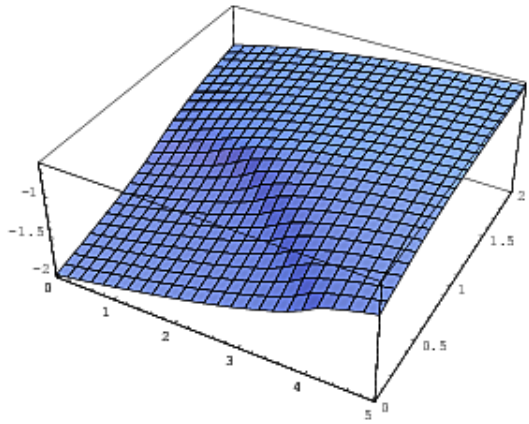

Fig. 7. Natural logarithm of transmittance coefficient D_{T} in $2\kappa l_{\mathrm{ch}}/\rho_{\mathrm{b}}(0)$ units as a function of work parameter a and energy parameter ε. The range of a is from 0 to 5 and the range of ε is from 0 to 2. The inversion effect, also anticipated by the Smoluchowski approach (Sec. 3), is seen near the top of the curve.

- Variation of synovial fluid pH has strong implications for the electrical charge of both the SAPL and the interstitial matrices of AC thereby effecting frictional properties. The change of the electrical charge of the SAPL is due to hydrogen ion binding at specific phospholipid lamina sites, while for interstitial matrix surfaces, binding occurs within proteoglycan and collagen aggregates exposed by loss of SAPL coverage. For example, at typical physiologic ambient solution pH = 7.4, which

is above the resident molecules' isoelectric point (pI $\sim$ 4.2), SAPL and exposed interstitial matrix surfaces are both negatively charged [11]. This negative charge density increases with increasing ambient solution pH due to attendant protonation potentials. For juxtaposed SAPL membranes, such charge structure facilitates boundary lubrication due to weak adhesion forces (repulsive interaction) and a very low coefficient of friction (Fig. 6). Because protons have the highest charge-to-mass ratio present in the system, and considering their very rapid structural diffusion in aqueous environments, the MNET model predicts their role in decreasing interfacial friction under sufficient physiologic SAPL loading as consistent with other observations [35]. Further, during conditions utilizing media replacement of synovial fluid, such as during arthroscopic interventions, proton recruitment at 5.3×10^{11} during the positive portion of the physiochemical scalpels alternating current signal generates an irrigant proton pressure force of approximately 2.8 mmHg that is similar in magnitude to the transcapillary net filtration gradient required to generate normal net capillary filtration [3] and which is of a time integrated scale predicted in the MNET model to be manageable by normal SAPL functions during decreased loading environments.

- The relationships between solution pH and wettability (measured by the contact angle), interfacial energy, and friction coefficient of a weak polyelectrolyte phospholipid bilayer-membrane could insight into the mechanisms underlying lubrication processes in mammalian joints. It has been shown [35] that the combination of a low interfacial energy and large contact angle provides effective biological lubrication. The significant contribution of phospholipids to the cartilaginous bearing includes: *(i)* a membrane for maintaining (weakly) slip plane bilayer lubricants to the joint cartilage [14], and *(ii)* liposomal synovial fluid and lamellar spheres which act also as lubricant support at the surface. The lamellar-roller-bearing lubrication model [35] has been developed to incorporate a bimodal mechanism of lamellar nearly frictionless bilayers movement and a roller-bearing lubrication mode through structured synovial complex-fluid [6] which occurs when lamellar spheres, liposomes, and macromolecules act as a roller-bearing [40] placed between two cartilage surfaces in biological lubrication.

- In very general conceptual terms, the MNET model illustrates that SAPL nanoscale channels are closed in the unloaded state and open in the loaded state, a finding in direct agreement with clinical observations [1–4]. For example, in the unloaded state such as during arthroscopic therapeutics, the SAPL serves as a charge barrier, a fea-

ture that has been used as a trait-targeting substrate to achieve the precision resection of physiochemical scalpels that utilize proton delivery gradients. Such charge barrier properties manifest under therapeutic conditions as the delivery gradients deployed in the form of engineered irrigants do not approach phase transition temperatures or ambient conditions associated with pore freezing phenomena [41]. Because SAPL coverage is related to interstitial matrix surface roughness, a feature corroborating the intuitive surgical desire to create a smooth AC surface, these proton delivery gradients are utilized to decrease the abnormal surface asperities typical of interstitial matrix failure. Although the SAPL is fundamental to a normal bearing surface, therapeutic interventions have only recently been focused upon its re-establishment. Full-thickness AC lesions have garnered significant attention, yet therapeutic efforts continue to struggle with host-implant lateral integration principally due to iatrogenic damage of the host interface at or within the wound bed. Accordingly, attention toward reconstituting a normal bearing [35] surface to facilitate outcome durability remains premature for full-thickness lesions. However, recent advances in tissue rescue for partial-thickness lesions have increased the awareness of re-establishing a normal SAPL bearing surface, most notably due to the ability to create a biologically responsive wound bed without margin collateral damage or phenotypic dedifferentiation and which displays a decrease in surface roughness amenable to SAPL reformation (self-assembly) once the treated surface is returned to an *in vivo* tribochemical interfacial synovial fluid milieu.

As a future task it is worth noticing that the interfacial [42] properties of hydrophilic biosurfaces exhibit an aqueous exclusion zone that has unique characteristics from that of bulk water and which are similar in nature to an electric double layer [1, 3, 15, 42]. The MNET model provides a foundation from which the mechanisms of exclusion zone and electric double layer formation can be studied. For example, biosurfaces have been generally examined in a fairly unloaded state [43] wherein phospholipid tissue membranes act as a charge barrier due to proton gradient formation secondary to augmented water dissociation. The MNET model depicts this condition in the right portions of Figs. 3 and 4 that represent the dominating electric force present and enhanced by geometric channel confinement. This type of unloaded condition at the SAPL is present during arthroscopic interventions with saline media replacement of synovial fluid. However, when placed under sufficient load, these phospholipid tissue membranes allow channel opening as depicted in the left portions of Figs. 3 and 4 that represent the enthalpic interplay between geometric and electrostatic confinement yielding proton wave inversions that enhance lubrication capabilities. Accordingly,

the MNET model describes the return of phospholipid tissue membranes such as the SAPL from saline media to an *in vivo* physiologically loaded synovial fluid environment post-treatment. Both of these loading conditions are supported by quantum mechanical evaluation. The whole argumentation addressed above, should be, however, left for another examination.

The project BS5/2009 at UTP Bydgoszcz, with a support to this study, is to be mentioned. The computers and software of Wrocław Metropolitan Supercomputing Centre (WCSS) were used in the study. A.G. and J.H. wish to thank Professor Z.J. Grzywna for many stimulating biophysical discussions.

REFERENCES

[1] W.K. Augé II, *Int. J. Nanosystems* **5**, 1 (2012).
[2] W.K. Augé II, *Osteoarthritis Cartilage* **20**, S147 (2012).
[3] W.K. Augé II, *Nano Energy* **1**, 309 (2012).
[4] K. Ganguly *et al.*, *Cartilage* **3**, 141 (2012).
[5] M. Daniel, in: *Advances in Planar Lipid Bilayers and Liposomes*, Ed. A. Iglic, Elsevier — Academic Press, Amsterdam 2012, pp. 225–243.
[6] A. Dedinate, *Soft Matter* **8**, 273 (2012).
[7] Z. Pawlak *et al.*, *Cell Biochem. Biophys.* **65**, 335 (2012).
[8] J. Seror, *Biomacromolecules* **13**, 3823 (2012).
[9] T.A. Schmidt, R.L. Sah, *Osteoarthritis Cartilage* **15**, 35 (2007).
[10] I.D. McRury, R.E. Morgan, W.K. Augé II, *Water* **2**, 108 (2010).
[11] A. Gadomski, Z. Pawlak, A. Oloyede, *Tribol. Lett.* **30**, 83 (2008).
[12] T.E. Decoursey, *Physiol. Rev.* **83**, 475 (2003).
[13] Z. Pawlak *et al.*, *Tribol. Intern.* **43**, 1719 (2010).
[14] Z. Pawlak *et al.*, *Acta Bioeng. Biomech.* **14**, 101 (2012).
[15] H. Yoo, R. Paranji, G.H. Pollack, *J. Phys. Chem. Lett.* **2**, 532 (2011).
[16] C.M. De Godoy, S. Cukierman, *Biophys. J.* **81**, 1430 (2001).
[17] M. Tuckerman, K. Laasonen, M. Sprik, M. Parrinello, *J. Chem. Phys.* **103**, 150 (1995).
[18] B. Chai, G.H. Pollack, *J. Phys. Chem. B* **114**, 5371 (2010).
[19] N. Agmon, *Chem. Phys. Lett.* **244**, 456 (1995).
[20] J.D. Bernal, R.H. Fowler, *J. Chem. Phys.* **1**, 515 (1933).
[21] B.E. Conway, J.O.M. Bockris, H. Linton, *J. Chem. Phys.* **24**, 834 (1956).
[22] C.J. Fecko *et al.*, *Science* **301**, 1698 (2003).
[23] N. Agmon, *Chem. Phys. Lett.* **319**, 247 (2000).

[24] V.I. Roldughin, *Russ. Chem. Rev.* **81**, 875 (2012).
[25] M. Doi, S.F. Edwards, *The Theory of Polymer Dynamics*, Clarendon Press, Oxford, 1986, chap. 3.
[26] D. Reguera, J.M. Rubí, J.M.G. Vilar, *J. Phys. Chem.* **B109**, 21502 (2005).
[27] I. Santamaría-Holek, J.M. Rubí, A. Pérez-Madrid, *New J. Phys.* **7**, 35 (2005).
[28] A. Plonka, *Dispersive Kinetics*, Kluwer, Dordrecht 2001.
[29] J.M. Rubí, D. Reguera, *Chem. Phys.* **375**, 518 (2010).
[30] S.H. Chung, S. Kuyucak, *Biochim. Biophys. Acta* **1565**, 267 (2002).
[31] A. Gadomski *et al.*, *Math. Biosc.* **244**, 188 (2013).
[32] G. Palladin, A. Vulpiani, *Phys. Rep.* **156**, 147 (1987).
[33] V.O. Kharchenko, I. Goychuk, *Phys. Rev.* **E87**, 052119 (2013).
[34] K. Ganguly *et al.*, *Cartilage* **1**, 306 (2010).
[35] Z. Pawlak, W. Urbaniak, A. Oloyede in: *Biomaterials and Medical Tribology: Research and Development*, Ed. J.P. Davim, Woodhead Publishing Reviews, Cambridge 2013, pp. 253–310.
[36] A.G. Cherstvy, A.B. Kolomeisky, A.A. Kornyshev, *J. Phys. Chem.* **B112**, 4741 (2008).
[37] A.G. Cherstvy, *Phys. Chem. Chem. Phys.* **13**, 9942 (2011).
[38] Z.J. Grzywna, J. Stolarczyk, *Acta Phys. Pol. B* **36**, 1595 (2005).
[39] Z.J. Grzywna, J. Stolarczyk, *Int. J. Mod. Phys.* **C13**, 1301 (2002).
[40] Z. Pawlak, A. Oloyede, *Biosystems* **94**, 193 (2008).
[41] J. Gallaher, K. Wodzinska, T. Heimburg, M. Bier, *Phys. Rev.* **E81**, 061925 (2010).
[42] A. Gadomski, J. Siódmiak, *Croat. Chem. Acta* **76**, 129 (2003).
[43] S.P. Singh, R.G. Winkler, G. Gompper, *Phys. Rev. Lett.* **107**, 158301 (2011).